Subwavelength silicon microcavities

Jeffrey Shainline[1]*, Stuart Elston[1], Zhijun Liu[2], Gustavo Fernandes[2], Rashid Zia[2] and Jimmy Xu[1,2]

[1]*Department of Physics, 184 Hope St., Brown University, Providence, RI 02912*
[2]*Division of Engineering, 184 Hope St., Brown University, Providence, RI 02912*
**jeffrey.shainline@gmail.com*

Abstract: We present a study of the first silicon microdisk resonators which are smaller than the free-space resonant wavelength in all spatial dimensions. Spectral details of whispering gallery modes with azimuthal mode number m = 4-7 are measured in microdisks with diameters between 1.35 and 1.89μm and are studied at wavelengths from 1.52 to 1.62μm. For the structures considered here, m = 5 is the highest azimuthal mode order in a subwavelength cavity and has measured Q = 1250. These results agree well with theoretical calculations using a finite difference frequency domain method and fit an exponential scaling law relating Q to disk radius via m.

OCIS codes: (230.5750) Resonators; (130.3990) Micro-optical devices.

References and links

1. S. L. McCall, A. F. J. Levi, R. E. Slusher, S. J. Pearton, and R. A. Logan, "Whispering-gallery mode microdisk lasers," Appl. Phys. Lett. **60**(3), 289–291 (1992).
2. A. F. J. Levi, R. E. Slusher, S. L. McCall, T. Tanbun-Ek, D. L. Coblentz, and S. J. Pearton, "Room temperature operation of microdisc lasers with submilliamp threshold current," Electron. Lett. **28**(11), 1010–1012 (1992).
3. A. F. J. Levi, S. L. McCall, S. J. Pearton, and R. A. Logan, "Room temperature operation of submicrometre radius disk laser," Electron. Lett. **29**(18), 1666–1667 (1993).
4. M. T. Hill, Y.-S. Oei, B. Smalbrugge, Y. Zhu, T. de Vries, P. J. van Veldhoven, F. W. M. van Otten, T. J. Eijkemans, J. P. Turkiewicz, H. de Waardt, E. J. Geluk, S.-H. Kwon, Y.-H. Lee, R. Nötzel, and M. K. Smit, "Lasing in metallic-coated nanocavities," Nat. Photonics **1**(10), 589–594 (2007).
5. Q. Song, H. Cao, S. T. Ho, and G. S. Solomon, "Near-IR subwavelength microdisk lasers," Appl. Phys. Lett. **94**(6), 061109 (2009).
6. C. Manolatou, and F. Rana, "Subwavelength nanopatch cavities for semiconductor plasmon lasers," IEEE J. Quantum Electron. **44**(5), 435–447 (2008).
7. Q. Xu, D. Fattal, and R. G. Beausoleil, "Silicon microring resonators with 1.5-microm radius," Opt. Express **16**(6), 4309–4315 (2008).
8. K. Srinivasan, P. E. Barclay, M. Borselli, and O. Painter, "Optical-fiber-based measurement of an ultrasmall volume high- Q photonic crystal microcavity," Phys. Rev. B **70**(8), 081306 (2004).
9. M. Eichenfield, R. Camacho, J. Chan, K. J. Vahala, and O. Painter, "A picogram- and nanometre-scale photonic-crystal optomechanical cavity," Nature **459**(7246), 550–555 (2009).
10. M. Borselli, K. Srinivasan, P. E. Barclay, and O. Painter, "Rayleigh scattering, mode coupling and optical loss in silicon microdisks," Appl. Phys. Lett. **85**(17), 3693–3695 (2004).
11. M. Borselli, T. J. Johnson, and O. Painter, "Beyond the Rayleigh scattering limit in high-Q silicon microdisks: theory and experiment," Opt. Express **13**(5), 1515–1530 (2005).
12. K. Srinivasan, M. Borselli, O. Painter, A. Stintz, and S. Krishna, "Cavity Q, mode volume, and lasing threshold in small diameter AlGaAs microdisks with embedded quantum dots," Opt. Express **14**(3), 1094–1105 (2006).
13. K. Zhang, and D. Li, *Electromagnetic Theory for Microwaves and Optoelectronics* (Springer, 1998).
14. J. E. Heebner, T. C. Bond, and J. S. Kallman, "Generalized formulation for performance degradations due to bending and edge scattering loss in microdisk resonators," Opt. Express **15**(8), 4452–4473 (2007).
15. Amnon Yariv, *Quantum Electronics* (John Wiley and Sons, 1989), Chap. 22.
16. Jens Uwe Nöckel, "Resonances in nonintegrable open systems," Ph.D. thesis (Yale University, 1997) pp 91–105.
17. R. P. Wang, and M.-M. Dumitrescu, "Optical modes in semiconductor microdisk lasers," IEEE J. Quantum Electron. **34**(10), 1933–1937 (1998).
18. N. C. Frateschi, and A. F. J. Levi, "The spectrum of microdisk lasers," J. Appl. Phys. **80**(2), 644 (1996).
19. P. Lusse, P. Stuwe, J. Schule, and H.-G. Unger, "Analysis of vectorial mode fields in optical waveguides by a new finite difference method," J. Lightwave Technol. **12**(3), 487–494 (1994).
20. R. Zia, M. D. Selker, and M. L. Brongersma, "Leaky and bound modes of surface plasmon waveguides," Phys. Rev. B **71**(16), 165431 (2005).
21. H. Benisty, J.-M. Gerard, R. Houdre, J. Rarity, and C. Weisbuch, eds., *Confined Photon Systems* (Springer, New York, 1998).

#118169 - $15.00 USD Received 5 Oct 2009; revised 6 Nov 2009; accepted 25 Nov 2009; published 4 Dec 2009

22. B. Min, E. Ostby, V. Sorger, E. Ulin-Avila, L. Yang, X. Zhang, and K. Vahala, "High-Q surface-plasmon-polariton whispering-gallery microcavity," Nature **457**(7228), 455–458 (2009).
23. A. C. F. Hoole, M. E. Welland, and A. N. Broers, "Negative PMMA as a high-resolution resist—the limits and possibilities," Semicond. Sci. Technol. **12**(9), 1166–1170 (1997).
24. L. Deych, and J. Rubin, "Rayleigh scattering of whispering gallery modes of microspheres due to a single scatterer: myths and reality." arXiv:0812.4404v1 [physics.optics] 23 Dec 2008.

1. Introduction

Planar lightwave circuits face the challenge of entering a market dominated by electronics whose progress has been driven by Moore's law and the ability to fabricate consistently smaller transistors. For photonic circuits, a physical size constraint emerges; the characteristic limiting size is the wavelength of light traversing the circuit. To overcome this physical limitation a great deal of research has recently been conducted to explore the potential of structures at and below this size limit to store and generate light. Beginning with the original demonstration of wavelength-scale microdisk lasers [1–3], more recent demonstrations have shown that structures smaller than the wavelength of light in all three spatial dimensions can give rise to laser action at cryogenic temperatures [4–6]. Previous experimental studies of passive resonant cavities have explored ring resonators with diameters of approximately twice the free-space wavelength [7], but thorough comparison between theory and experiment has not yet been conducted for cavities smaller than the wavelength. Here we present a study of such subwavelength cavities using tapered optical fibers as the experimental probe. While photonic crystal cavities with mode volumes smaller than the wavelength have been probed with tapered fiber spectroscopy [8,9], these structures are by definition many wavelengths in size in at least one spatial dimension. Several tapered fiber studies of microdisks have been performed on passive silicon microcavities [10,11] as well as on active compound semiconductor cavities [12]. The subwavelength silicon microdisks studied in the present work are smaller than the free-space wavelength of light being stored in the cavity in all spatial dimensions and are much smaller in the axial dimension. To our knowledge, these resonators are, to date, the smallest resonant structures to be probed with tapered fiber spectroscopy or directly coupled to a waveguide. However, the spatial localization necessarily comes with a broadening in momentum space and reduced photon lifetime.

In this work we studied silicon microdisks of diameters ranging from smaller to larger than the wavelength corresponding to resonances of azimuthal mode number (m) from 2 to 7 with resonant wavelengths from 1.52μm to 1.62μm. We have quantified the relationship between the radiation-limited quality factor (Q) and m using tapered fiber spectroscopy and compared our results to finite-difference frequency-domain (FDFD) simulations. The m = 5 mode was the mode of highest m in a subwavelength disk and was measured to have radiation-limited Q = 1250, indicative of strong potential for room-temperature laser operation if fabricated from or coupled to a gain medium.

2. Theoretical considerations

Resonances in microdisks can be classified according to three mode numbers corresponding to quantization in the vertical, radial and azimuthal directions [13]. To completely specify the mode one must also specify the polarization as TE-like (H_z is the dominant field component) or TM-like (E_z is the dominant field component). The highest-Q resonances occur when the wave vector is predominantly in the azimuthal direction [14]. Therefore, we consider only modes of fundamental order in the vertical and radial direction and classify modes by m. Further, the partial differential equation describing the system is separable if one assumes $\exp(im\varphi)$ angular dependence and in the approximation that modes have purely TE or TM character. The equation governing the z-dependence is identical to that of a slab waveguide [15]. If one chooses $-\beta^2$ as the separation constant for the equation governing z-dependence (so the functional dependence on z inside the disk is $\cos\beta z$ for even modes), then $\beta = k_0(n^2 - \overline{n}^2)^{1/2}$, where k_0 is the free space spatial frequency, n is the index of refraction of the disk (taken to be 3.48 throughout this study), and $\overline{n}$ is the effective index of

#118169 - $15.00 USD Received 5 Oct 2009; revised 6 Nov 2009; accepted 25 Nov 2009; published 4 Dec 2009

refraction which enters the radial equation. Satisfying the boundary conditions at the top or bottom of the disk leads to the transcendental equation

$$\sqrt{n^2-\overline{n}^2}\,\tan\left(\frac{k_0 h}{2}\sqrt{n^2-\overline{n}^2}\right)=\xi\sqrt{\overline{n}^2-1} \tag{1}$$

where h is the thickness of the silicon disk and $\xi = n^2$ for TM modes and unity for TE modes. For a silicon disk of thickness h = 250nm operating at λ = 1550nm, $\overline{n}$ = 2.015 (2.914) for TM (TE) modes. The objective of this study was to explore the regime where the size of the disk is smaller than the free space wavelength. To this end, the substantially larger effective index for TE modes is an indispensable attribute. For this reason we consider only TE modes in this study. For sufficiently thin disks ($h \lesssim 300$nm) at $\lambda \approx 1550$nm, TE modes have significantly larger radiation-limited quality factors, have larger m for a given disk radius, and therefore all modes populating thin subwavelength disks are TE-polarized.

Having obtained the effective index of refraction through consideration of the z equation alone, the radial equation reads

$$-\frac{1}{r}\frac{d}{dr}r\frac{d}{dr}R(r)+V_{\text{eff}}(r)R(r)=k_0^2R(r), \tag{2}$$

where

$$V_{\text{eff}}(r)=k_0^2[1-\overline{n}^2(r)]+\frac{m^2}{r^2}. \tag{3}$$

The solution to Eq. (2) inside the disk is a Bessel function, $J_m(Tr)$, where $T=\overline{n}k_0$, $k^2=T^2+\beta^2$ and $k=nk_0$. The effective index of refraction, which enters Eq. (2) through Eq. (3), is a function of r in that it changes abruptly from its value inside the disk [determined by solution of Eq. (1)] to unity beyond the disk. It is this abrupt change which produces a potential well in which the electromagnetic field is contained. In Eq. (2) we have written Bessel's equation in a non-standard form to make an analogy to a one-dimensional Schrödinger equation. In this analogy, k_0^2 plays the role of the energy eigenvalue of the quantum eigenstate. The limit of the analogy is that k_0^2 also enters into the effective potential. Special consideration of the curvilinear kinetic energy term must be given if one is to justify the definition of the effective potential as in Eq. (3). Discussion of this point is held in Ref [16]. Further consideration of the effective potential picture as applied to microdisks is given in Section 5.

In order to make quantitative predictions about the microdisk modal characteristics, we have used both analytical and numerical methods. Specifically, we investigated the analytical dispersion relations for microdisk whispering gallery modes by solving the appropriate boundary value problem [13–18], and we calculated the quasinormal modes of microdisk resonators using an FDFD mode solver. Adapting the approach described in Refs. [19] and [20], these FDFD calculations leveraged the azimuthal symmetry of the modes (i.e. the exp($im\varphi$) dependence) to semi-analytically reduce the 3D resonator geometry to a transverse 2D eigenvalue problem. This full-vectorial method allowed for calculations of all electromagnetic field components as well as the effective mode volume [12], Purcell enhancement [21] and bending-limited finesse [14]. Although this technique allows for adaptive meshing, a simple Cartesian mesh proved suitable for our calculations. A 10nm grid was utilized for all simulations. Convergence was observed as a function of simulation area. An index of refraction of 3.48 was used to model the silicon disks.

#118169 - $15.00 USD Received 5 Oct 2009; revised 6 Nov 2009; accepted 25 Nov 2009; published 4 Dec 2009

3. Fabrication of subwavelength silicon microdisks

Several techniques for fabricating microdisks result in angled sidewalls [8,11,22]. In some cases the angled sidewalls arise from fabrication steps which produce smoother sidewalls. Smooth sidewalls are of critical importance for microdisks which are not operating in the radiation-limited-Q regime, as Rayleigh scattering from sidewall imperfections is usually the dominant loss mechanism in such disks [11]. However, our theoretical and experimental experience informs us that in the subwavelength regime sidewall verticality is a greater concern than minor sidewall roughness. Silicon microdisks were fabricated on SOI (250nm silicon layer, 3μm buried oxide). To make disks with sidewalls which are vertical and yet as smooth as possible we perform negative electron beam lithography with PMMA [23] at a dosage of $2x10^4$μC/cm^2. At dosages of this magnitude, the polymer units of PMMA crosslink to form a material which is resistant to etchants. In our experiments, this technique has given smoother sidewalls than simply performing positive lithography without resist reflow. The electron exposure is followed by development in acetone and ICP RIE with SF_6 and C_4F_8. Photolithography and deep ICP RIE are then performed to etch through the 3μm SiO_2 insulator layer and through ~30μm of the underlying silicon substrate. This isolates the disks on a strip which is lifted above the rest of the substrate and thus makes it easier access the disks with the tapered fiber. An undercut is performed with buffered hydrofluoric acid.

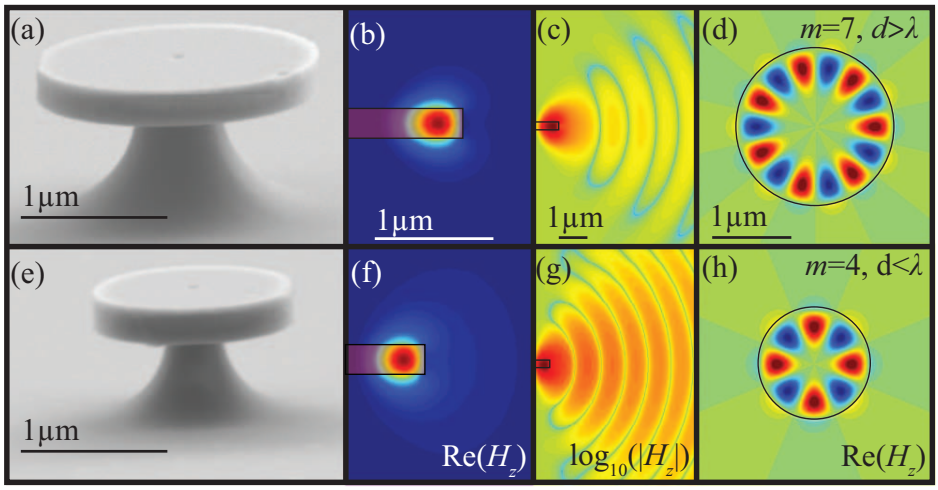

Fig. 1. Fabricated structures and calculated field profiles of microdisks for m = 7 and m = 4 modes. a) Disk of 1.89μm diameter. b) Re(H_z) field profile of m = 7 mode in the y-z plane calculated with the FDFD method. Q = 18,200. c) Far field ($\log_{10}(|\mathrm{Re}(H_z)|)$) for the same disk. d) Re(H_z) in the x-y plane calculated analytically. e) Disk of 1.35μm diameter. f-h) Calculations for the 1.35μm disk corresponding to those in b-d.

SEM images of two completed disks are shown in Fig. 1 along with the calculated near- and far-field profiles of their resonant modes. Contrasting Fig. 1(b) and Fig. 1(f) one sees the near-field amplitude extending further radially and axially in the subwavelength disk. Contrasting Fig. 1(c) and Fig. 1(g) one observes the increased far-field radiation emanating from the subwavelength cavity.

4. Experimental details and results

To experimentally characterize the disks we utilize the technique of tapered fiber spectroscopy [8–12]. A tunable laser sweeps the wavelength range from 1.52μm to 1.62μm. The transmission through a tapered fiber coupled to a disk is monitored with an optical spectrum analyzer. The transmission dips are fit to a Lorentzian function and the Q factor is extracted from the width and center wavelength.

#118169 - $15.00 USD Received 5 Oct 2009; revised 6 Nov 2009; accepted 25 Nov 2009; published 4 Dec 2009

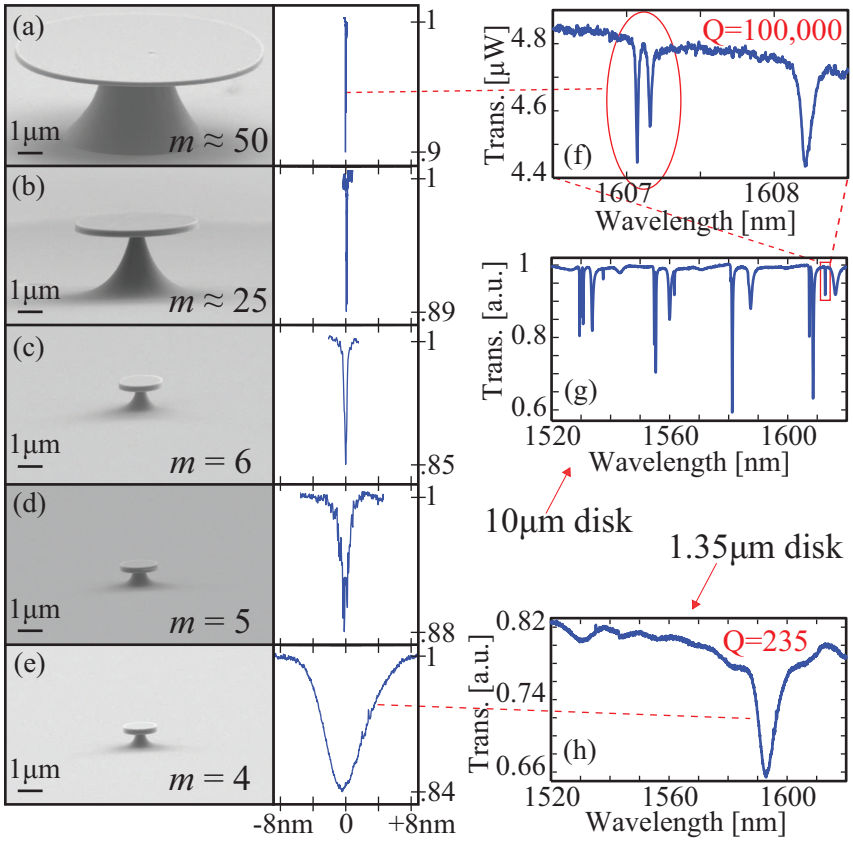

Fig. 2. Silicon microdisks of decreasing diameters and tapered fiber spectra. a-e) SEM images of disks of diameter 10μm, 5μm, 1.75μm, 1.48μm and 1.35μm respectively. Resonant transmission dips in tapered fiber spectra acquired from the disks are shown. The *y*-axes of these plots are transmission in arbitrary units and the *x*-axis is wavelength detuning. f) High resolution tapered fiber spectrum of a 10um disk. g) Scan of the full tunable laser range for the 10mm disk. h) Scan of the full tunable laser range for the m = 4 mode.

Figure 2 shows SEM images of microdisks with diameters varying from 10μm—with radiation-limited Q on the order of 10^{13} (the Rayleigh-scattering-limited Q in this disk is ~10^5)—down to a subwavelength disk of approximately 1μm diameter with radiation-limited Q = 235. Next to each disk is a tapered fiber spectrum of the characteristic resonance of the disk. The SEM images depict the decrease in size over an order of magnitude while broadening of the resonances demonstrates the exponential decrease in Q factor. In Figs. 2(f)-2(h) tapered fiber spectra of large and small disks are contrasted in more detail. Figure 2(f) shows a high-resolution scan of a 2nm wavelength window of a tapered fiber spectrum from a 10μm-diameter silicon disk. The doublet character of the high-Q mode is apparent, as discussed in Refs. [10–12,24]. Figure 2(g) shows a scan of the entire tunable laser range for the same disk. The free spectral range is ~27nm. Several families of modes are present, and in addition to the highest-Q, fundamental-radial-order modes, lower-Q, higher-radial-order modes are present. In Fig. 2(h) a tapered fiber spectrum of a 1.35μm disk is shown. The free spectral range is ~200nm, and only one resonance is present. If one wishes to use whispering-gallery-mode microcavities for devices such as filters and switches, the large free spectral range of wavelength-scale microdisks is an attractive feature. Another attribute is that higher-radial-order modes do not exist in this wavelength range for a disk of this size. The other features of the spectrum in Fig. 2(h) are due to coupling to the substrate. Because these small disks are only a few hundred nanometers from the substrate, coupling of the fiber to the substrate is more prominent than in larger disks.

#118169 - $15.00 USD Received 5 Oct 2009; revised 6 Nov 2009; accepted 25 Nov 2009; published 4 Dec 2009

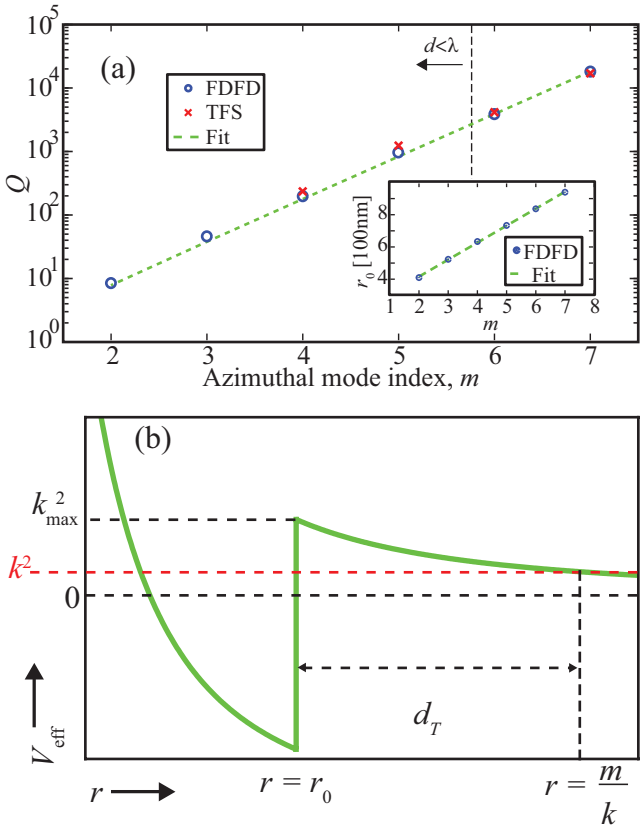

Fig. 3. Microdisk Q versus m. a) Experimental data, theoretical values obtained with FDFD and a fit to an exponential function are shown. The linear relationship between the disk radius, r_0, and m is shown in the inset. b) The effective potential and tunneling parameters.

In Fig. 3 we present a comparison of the experimentally-obtained Q factors with the theoretical radiation-limited Q factors obtained with FDFD calculations. The experimental points are acquired using tapered fiber spectroscopy as described above, and the theoretical points are determined by using the values of disk diameter as measured with SEM in the FDFD mode solver. The thickness of each disk was 250nm. The data for each azimuthal mode order is from a disk of a different radius so the resonant wavelengths are nearly equal. The agreement between experiment and theory indicates that our silicon microdisks have radiation-limited Q factors that are not significantly degraded by minor sidewall perturbations. It should be noted that the measured resonance at $m = 7$ was a doublet mode. The splitting was only observed for the $m = 7$ mode where the Lorentzian is narrow enough to differentiate the two peaks. We find that the $m = 5$ mode is the subwavelength mode of highest m with measured $Q = 1250$. The diameter of the disk was 1.49μm and resonant wavelength was 1.543μm giving a ratio of $d/\lambda = 0.967$. The $m = 4$ mode was observed in a cavity of diameter 1.35μm at wavelength of $\lambda = 1.591$μm giving $d/\lambda = 0.849$. Due to the limited wavelength window accessible by our tunable laser, and the broad nature of the low-Q $m = 3$ mode, it was not observed in our studies. The theoretical value of $d/\lambda = 0.683$ for the $m = 3$ mode. Below $m = 3$ the resonances have $Q < 10$. To create microdisks with well defined resonances for $m < 3$ and $d/\lambda < 0.7$, metallodielectric architectures, which trade ohmic loss for suppressed radiation, may offer advantages [4,6,22].

#118169 - $15.00 USD Received 5 Oct 2009; revised 6 Nov 2009; accepted 25 Nov 2009; published 4 Dec 2009

Table 1. Theoretical and measured microdisk modal parameters

m	r_{meas}	r_{sim}	λ_{meas}	λ_{sim}	Q_{meas}	Q_{sim}	υ_{eff}
7	0.945μm	0.946μm	1.530μm	1.555μm	17,000	18,200	3.07
6	0.877μm	0.876μm	1.589μm	1.621μm	4160	3834	2.61
5	0.743μm	0.746μm	1.543μm	1.581μm	1253	1010	2.21
4	0.675μm	0.676μm	1.591μm	1.617μm	235	198	1.80
3	*	0.536μm	*	1.569μm	*	47.6	1.52
2	*	0.416μm	*	1.558μm	*	8.72	1.18

For more direct comparison between experiment and theory, we also present the data in Table 1. The radii of the disks, as measured with SEM, the measured resonant wavelengths, and the measured quality factors obtained by fitting the transmission spectra to a Lorentzian function are listed alongside the theoretical values obtained from the FDFD simulations. In addition, the calculated effective mode volumes are given in Table 1. The effective mode volume is calculated from the formula

$$\upsilon_{eff} = \frac{\int \epsilon(\mathbf{r}) \mid E(\mathbf{r}) \mid^2 d^3\mathbf{r}}{\max[\epsilon(\mathbf{r}) \mid E(\mathbf{r}) \mid^2]}. \quad (4)$$

To calculate the volume integral in the numerator of Eq. (4), $\exp(im\varphi)$ angular dependence is assumed, as it was to arrive at Eq. (2). This is an important distinction when contrasted with the work of Ref. [12] wherein standing waves with $\sin(m\varphi)$ angular dependence are assumed. The mode volume calculated assuming standing waves is half that of the circulating waves. In light of the work in Ref. [24] there does not seem to be justification for assuming the circularly-propagating waves injected into the microcavity from the tapered fiber establish standing waves when scattered from sidewall imperfections. To calculate the values of the effective mode volume presented in Table 1, the integral in Eq. (4) was performed over the entire simulation space which extended 2μm above and below the disk and 6μm in the radial direction.

In using evanescent coupling in transmission measurements to determine the radiation-limited Q of a resonator it is important to consider other loss mechanisms contributing to the measured Q. The relation between the various contributions to cavity loss can be expressed as

$$Q_{meas}^{-1} = Q_{rad}^{-1} + Q_c^{-1} + Q_p^{-1}, \quad (5)$$

where the three contributions to the measured quality factor are radiation, coupling to the tapered fiber waveguide and parasitic losses such as sidewall scattering. In the structures considered here, $Q_{rad} < 20{,}000$, and Q_p in larger disks fabricated with similar methods has been measured to be greater than 100,000. For this reason it is justified to neglect the contribution from Q_p in Eq. (5). Q_c is a function of the gap between the resonator and the waveguide, and this fact can be exploited to determine the relative contributions to Eq. (5) from Q_{rad} and Q_c. In the experiments performed in this study, the tapered fiber position relative to the disk was controlled with 100nm resolution. As can be seen in Fig. 1, the near field of the modes decays over 1-2μm. To accurately determine Q_{rad}, transmission spectra were taken with the fiber very near the disk to determine resonance positions. The fiber was then incrementally moved away from the disk, and additional spectra were acquired as the gap between the fiber and disk was increased. As in Ref. [10], increasing the gap resulted in a decrease in the depth of the transmission dip and increase in the measured Q. Convergence behavior was observed until the depth of the dip was at the level of the measurement noise; the reported values for Q_{meas} in Fig. 3 and Table 1 are those from the maximal fiber-disk gap which resulted in a value consistent with the convergence trend and with a deep enough dip to be fit to a Lorentzian. We did not directly measure the fiber-resonator gap because in

#118169 - $15.00 USD Received 5 Oct 2009; revised 6 Nov 2009; accepted 25 Nov 2009; published 4 Dec 2009

measurements of such small disks so close to the substrate it is advantageous to hold the fiber above the plane of the disk, and the devices were only viewed directly from above.

It is important to note that contributions to error in the tapered fiber measurements are numerous. They include coupling between the fiber and disk, noise due to vibrations of the fiber, substrate and disk coupling and perturbation due to the pedestal. Additionally, uncertainty in the measurement of disk diameters with SEM affects comparison between experiment and theory. Because the contributions to error are so varied and each is so difficult to quantify, we do not venture to guess at the uncertaintly in the data in Table 1. We note that measured resonant wavelengths are within 1-3% of predicted values, measured Q factors are near 10-20% of predicted values, and this is true with or without consideration of the substrate and pedestal in the model. For the lower azimuthal mode numbers, the measured values are consistently higher than the theoretical values, indicating a tendency of the FDFD mode solver to underestimate the radiation-limited Q.

The effect of the substrate is more pronounced if one considers non-undercut resonators in this low-m regime. The theoretical values of the m = 4 device listed in Table 1 if the entire half space below the disk is filled with dielectric characterized by n = 1.46 are Q_{sim} = 104 and λ_{sim} = 1.630μm. For the m = 7 disk with no undercut Q_{sim} = 5265 and λ_{sim} = 1.555μm.

5. Analysis

Analysis of our data reveals that m has a linear relationship with r_0 over the range m = 2-7 at a (nearly) constant wavelength. Q has an exponential dependence on m of the form $Q(m) = A \exp(\chi m)$, where A = 0.374 and χ = 1.54 are parameters which have been determined with non-linear regression. As seen in Fig. 3, this expression fits our data quite well over the range of m values considered here. The linear dependence of m on r_0 can be understood because the mode propagates around the circumference of the disk. The effective mode volume also has a linear dependence on m. Thus, the Purcell enhancement decays exponentially with decreased m, as does the finesse [14].

The exponential dependence of Q on m can be understood in the framework of the effective potential [16,18], which is given by Eq. (3) and is plotted in Fig. 3(b). This quantity enters the scalar radial equation for the dominant field component if TE or TM polarization is assumed. As discussed in Sec. 2, V_{eff} changes discontinuously at the edge of the disk, creating a potential well in which the electromagnetic field predominantly resides. There are two features of a potential which affect the tunneling probability: the barrier height and barrier width. For a given wavelength, the height of the tunneling barrier scales as m^2/r_0^2. In a general one-dimensional tunneling scenario, the tunneling probability will have a power law dependence on barrier height. Therefore, the quadratic dependence of the barrier height on m cannot explain the exponential dependence of Q on m. However, the tunneling probability through a one-dimensional barrier is exponentially dependent on the barrier width. As shown in Fig. 3, the radial distance at which the confined mode can emerge to free space is $r = m/k$, and is determined by the condition $V_{eff} = k^2$. Thus, the tunneling barrier thickness is given by $d_T = m/k - r_0$. Using the linear relationship between m and r_0 ($r_0 = sm + b$) the tunneling thickness is $d_T = (1/k - s)m - b$. Thus,

$$\frac{1}{Q(m)} \propto T(m) \propto \exp[-\kappa d_T(m)] \propto \exp(-\kappa' m), \tag{6}$$

Where T is the tunneling probability and κ and κ'are unknown constants which could be determined from a rigorous treatment. Thus, the exponential dependence of Q on m (and r_0) is consistent with the linear dependence of tunneling barrier width on m.

6. Conclusions

In conclusion, we have investigated the resonant modes of silicon microdisks that are smaller in every dimension than the free-space wavelength of light being stored in the cavities. We have presented a systematic characterization of the m = 2-7 modes and have quantified the linear relationship between m and r_0 as well as the exponential dependence of Q on m. Our

#118169 - $15.00 USD Received 5 Oct 2009; revised 6 Nov 2009; accepted 25 Nov 2009; published 4 Dec 2009

experimental data is in agreement with theoretical values for the radiation-limited Q. We have demonstrated the m = 5 mode is the highest-Q mode in a subwavelength disk and was measured in our structures to have a Q = 1250 at a wavelength of 1.543μm in a microdisk of diameter 1.490μm.

Acknowledgements

We are grateful to Dr. Gernot Pomrenke and the grant support of AFOSR (FA9550-07-1-0286) and to the WCU program at SNU, Korea.

#118169 - $15.00 USD Received 5 Oct 2009; revised 6 Nov 2009; accepted 25 Nov 2009; published 4 Dec 2009